COMPUTER METHODS IN APPLIED MECHANICS AND ENGINEERING 22 (1980) 289–308

THREE-DIMENSIONAL ANALYSIS OF NONLINEAR MAGNETODYNAMIC FIELDS IN A SATURABLE REACTOR

Yoshifuru SAITO

Department of Electrical Engineering, College of Engineering, Hosei University, 3-7-2 Kajinocho Koganei, Tokyo 184, Japan

Manuscript received 16 November 1978
Revised manuscript received 27 August 1979
Second revision received 13 November 1979

The nonlinear magnetodynamic fields in a saturable reactor are calculated by the method of magnetic circuits, taking into account the eddy currents.

Notation

$\boldsymbol{C}$ magnetic flux connection matrix
$\boldsymbol{D}$ magnetic resistance matrix
$\mathrm{d}a$ infinitesimally small area
$\mathrm{d}l$ infinitesimally small distance
$\mathrm{d}/\mathrm{d}t$ time derivative
$\boldsymbol{E}$ $=\{e_1, 0, 0, 0\}$, externally impressed voltage vector
e externally impressed voltage [V]
$\boldsymbol{F}$ $=\left[\frac{N_1 e_1}{r_1}, 0, 0, 0\right]$, externally impressed magnetomotive force vector
$\boldsymbol{G}$ $=\left[\frac{1}{r_1}, 0, \frac{1}{r_3}, \frac{1}{r_4}\right]$, electrical conductance matrix
g mesh spacing in direction of y-axis
H magnetic field intensity [AT/m]
h mesh spacing in direction of x-axis
$\boldsymbol{I}$ $=\{i_1, i_2, i_3, i_4\}$, current vector
i current [A]
j current density [A/m^2]
$\boldsymbol{L}$ $=\left[\frac{N_1^2}{r_1}, 0, \frac{1}{r_3}, \frac{1}{r_4}\right]$, coefficient matrix
N_1 number of turns of the exciting coil
n unit normal vector
$R_{i\pm1/2}, R_{j\pm1/2}$ magnetic resistances around the mesh point (i, j)
$R_i^{(1)}, R_j^{(1)}$ magnetic resistances as function of permeability $\mu_{i+1,j}^{(1)}$ in direction of x-axis and of y-axis, respectively
$R_{i+1}^{(3)}$ magnetic resistance as function of permeability $\mu_{i+1,j}^{(3)}$ in direction of x-axis
$R_{j-1}^{(2)}$ magnetic resistance as function of permeability $\mu_{i,j-1}^{(2)}$ in direction of y-axis
r electric resistance [Ω]
$S_{i,j}$ surface area bounded by contour abcd
t time [sec]
$\boldsymbol{U}$ $=\{u_1, u_2, u_3, u_4\}$, induced voltage vector

u induced voltage [V]
$V_{i,j}^{(1)}$ volume of region taking permeability $\mu_{i,j}^{(1)}$
$\boldsymbol{W}$ $= [N_1, 1, 1, 1]$, winding matrix
w magnetic field energy [J]
$\boldsymbol{Z}$ $= \boldsymbol{D} + (\mathrm{d}/\mathrm{d}t)\boldsymbol{L}$, magnetic impedance matrix
α parameter of the finite difference method
Δt stepwidth [sec]
μ $= f(H)$, permeability as function of magnetic field intensity H
$\boldsymbol{\Phi}$ $= \{\phi_1, \phi_2, \phi_3, \phi_4\}$, magnetic flux vector
ϕ magnetic flux [Wb]

Superscripts 1, 2, 3, 4 refer to the permeabilities $\mu^{(1)}$, $\mu^{(2)}$, $\mu^{(3)}$, $\mu^{(4)}$; and t refers to the transpose of a matrix; and c refers to transformed quantities.
Subscripts i, $i \pm 1$, $i \pm 1/2$, j, $j \pm 1$, $j \pm 1/2$ refer to the positions x_i, $x_i \pm h$, $x_i \pm h/2$, y_j, $y_j \pm g$, $y_j \pm g/2$; t, $t + \Delta t$, $t + \Delta t/2$ indicate the time t, $t + \Delta t$, $t + \Delta t/2$; and 1, 2, 3, 4, 5 refer to the first, second, third, fourth, fifth elements of a saturable reactor, respectively.
Moreover, abcd, eb and bf denote the contour lines.

1. Introduction

The calculation of magnetic fields is of the utmost importance in the design of electromagnetic devices (e.g. transformers and electrical rotating machines). Because of the nonlinear magnetization characteristic of iron, it is extremely difficult to develop an analytical method for finding the magnetic fields in electromagnetic devices.

Conventional design methods for electromagnetic devices are based to a considerable extent on classical magnetic circuit theory and experience. Therefore, these design methods are incapable of determining the dynamic performance of electromagnetic devices.

With the development of modern computers, numerical methods became available to calculate the magnetic fields of electromagnetic devices, taking into account the nonlinear magnetization characteristic of iron. The numerical methods are fundamentally divided into two classes: (1) the finite difference method, which replaces partial derivatives by divided differences, and (2) the finite element method, which is based on variational formulations [1]–[7].

The author has reported that the method of magnetic circuits developed for a two- or three-dimensional space is one of the finite difference schemes in nonlinear magnetostatic field problems [8], [9].

The purpose of the present paper is to develop the method of magnetic circuits as a means of calculating three-dimensional magnetodynamic fields in a saturable reactor, taking into account the eddy currents.

2. Fundamental equations

2.1. Fundamental equations based on magnetic circuits

Consider the region bounded by the contour abcd in fig. 1a. It is possible to write the

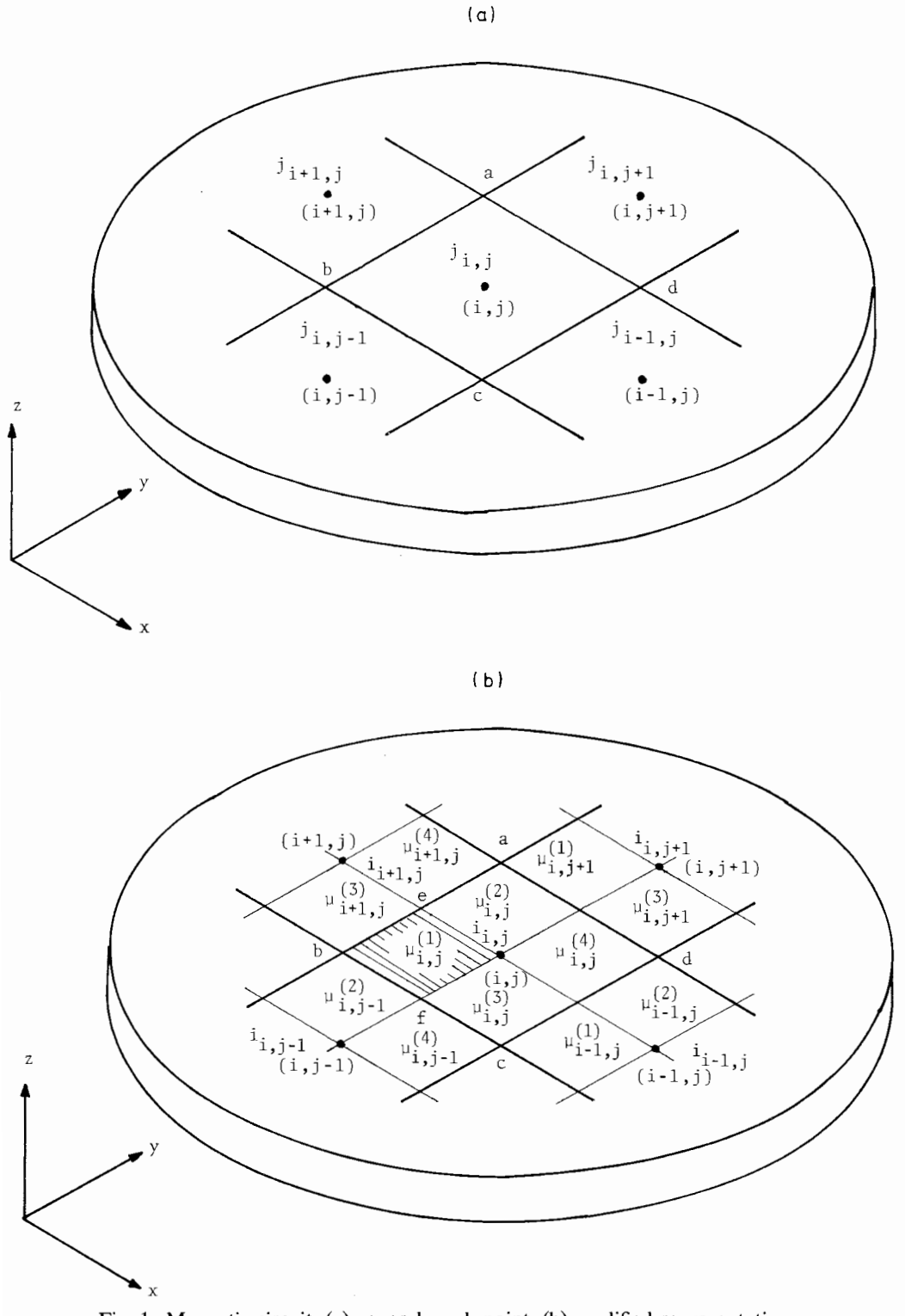

Fig. 1. Magnetic circuit. (a) general mesh point, (b) modified representation.

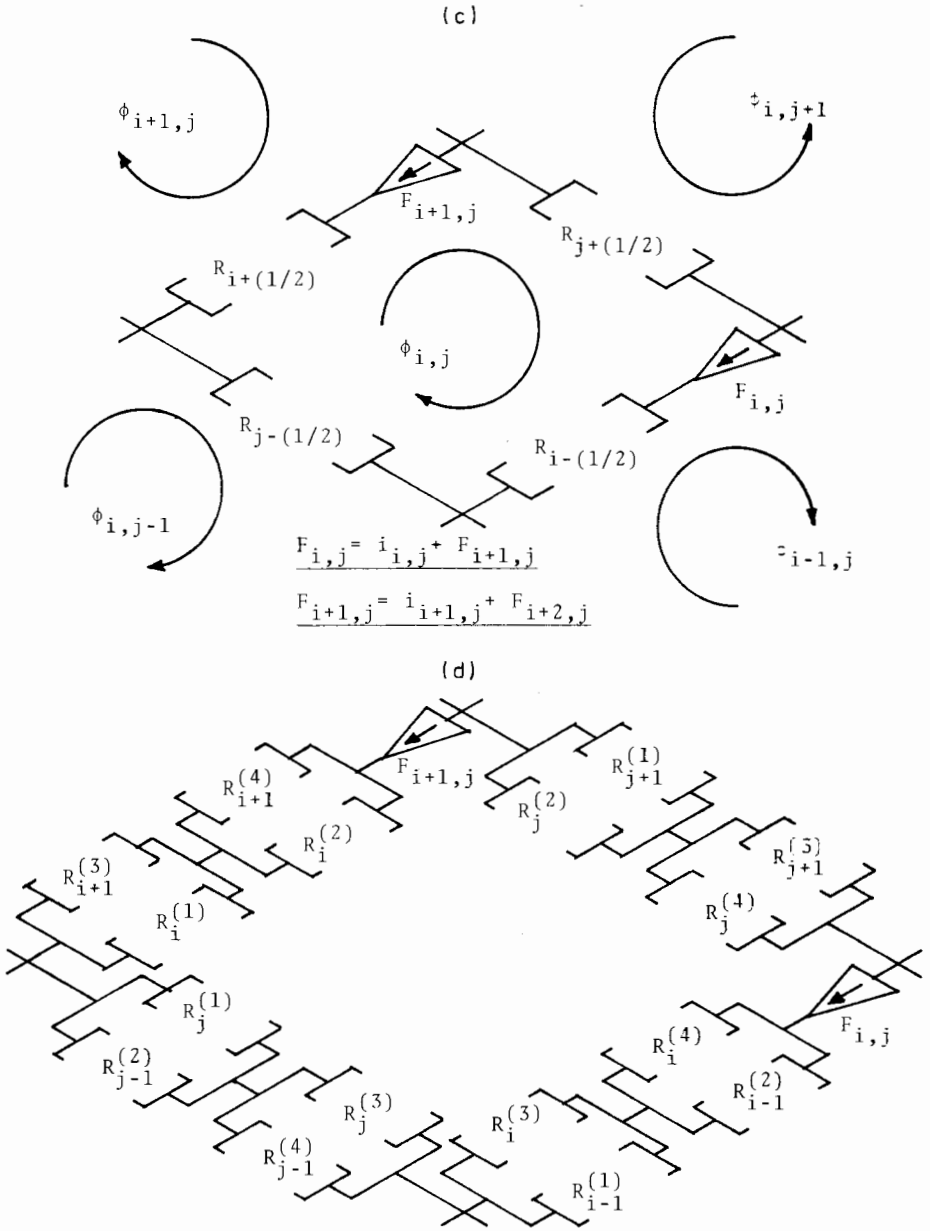

Fig. 1. Magnetic circuits. (c) circuit representation ($F_{i,j}$, F_{i+1}, denote the magnetomotive forces), (d) details of circuit.

fundamental relation between the magnetic field intensity H and current density $j_{i,j}$ as

$$\int_{\text{abcd}} H \, \mathrm{d}l = \int_{S_{i,j}} j_{i,j} n \, \mathrm{d}a, \tag{1}$$

where $\mathrm{d}l$ denotes the infinitesimally small distance along the contour abcd, $\mathrm{d}a$ is the infinitesimally small area, $S_{i,j}$ is the surface area bounded by the contour abcd, and n is the

unit normal vector on the infinitesimally small area da. Moreover, the subscripts i, j refer to the mesh point in fig. 1a. The right-hand term in eq. (1) is equivalent to the current $i_{i,j}$ through the surface $S_{i,j}$, viz.

$$\int_{S_{i,j}} j_{i,j} n \, \mathrm{d}a = i_{i,j}. \tag{2}$$

In order to apply the method of magnetic circuits to the region bounded by the contour abcd in fig. 1a, it is assumed that the current $i_{i,j}$ in eq. (2) is not uniformly distributed on the surface $S_{i,j}$ but concentrated on the conductor with infinitesimally small cross-sectional area located at the mesh point (i, j) in fig. 1a. Similarly, it is assumed that the currents in the other regions in fig. 1a are concentrated on the conductors with infinitesimally small cross-sectional area located at each of their mesh points.

Due to the nonlinear magnetization characteristic of iron, the permeability μ at each position takes different value with respect to the position. Therefore, it is assumed that the region which encloses these mesh points in fig. 1a is divided into four subdivisions in each of which the permeability μ may have a distinct value.

With these assumptions the magnetic fields in fig. 1a may be calculated for a modified form in the region as shown in fig. 1b. This means that the calculation can be carried out by the method of magnetic circuits, taking into account the nonlinear magnetization characteristic of iron.

In fig. 1b let $\phi_{i,j}$, $\phi_{i+1,j}$, $\phi_{i-1,j}$, $\phi_{i,j+1}$, $\phi_{i,j-1}$ denote the loop magnetic fluxes enclosing each of their mesh points, and let $R_{i+1/2}$, $R_{i-1/2}$, $R_{j+1/2}$, $R_{j-1/2}$ denote the magnetic resistances around the mesh point (i, j); then the left-hand term in eq. (1) is formally written as

$$R_{i+1/2}(\phi_{i,j} - \phi_{i+1,j}) + R_{i-1/2}(\phi_{i,j} - \phi_{i-1,j}) + R_{j+1/2}(\phi_{i,j} - \phi_{i,j+1})$$

$$+ R_{j-1/2}(\phi_{i,j} - \phi_{i,j-1}) = \int_{\mathrm{abcd}} H \, \mathrm{d}l, \tag{3}$$

where the loop magnetic fluxes $\phi_{i,j}$, $\phi_{i+1,j}$, $\phi_{i-1,j}$, $\phi_{i,j+1}$, $\phi_{i,j-1}$ are taken positive in the clockwise direction as shown in fig. 1c.

By means of eqs. (1)–(3) it is possible to represent the magnetic circuit equation as

$$R_{i+1/2}(\phi_{i,j} - \phi_{i+1,j}) + R_{i-1/2}(\phi_{i,j} - \phi_{i-1,j}) + R_{j+1/2}(\phi_{i,j} - \phi_{i,j+1})$$

$$+ R_{j-1/2}(\phi_{i,j} - \phi_{i,j-1}) = i_{i,j}. \tag{4}$$

However, under the dynamic conditions the current $i_{i,j}$ in eq. (4) has to include the effect of time variation. Therefore, the current $i_{i,j}$ is divided into two components: One is the eddy current due to the rate of change of the magnetic flux $\phi_{i,j}$ in time t, and the other is produced by the externally impressed voltage $e_{i,j}$, that is

$$i_{i,j} = \frac{1}{r_{i,j}} [e_{i,j} - (\mathrm{d}/\mathrm{d}t)\phi_{i,j}], \tag{5}$$

where d/dt denotes the time derivative, and $r_{i,j}$ is the electric resistance defined in the direction of z-axis in fig. 1a.

When eq. (5) is substituted into eq. (4), then we can formally obtain the magnetic circuit equation in the dynamic state as

$$R_{i+1/2}(\phi_{i,j}-\phi_{i+1,j})+R_{i-1/2}(\phi_{i,j}-\phi_{i-1,j})+R_{j+1/2}(\phi_{i,j}-\phi_{i,j+1})$$

$$+R_{j-1/2}(\phi_{i,j}-\phi_{i,j-1})=\frac{1}{r_{i,j}}[e_{i,j}-(\mathrm{d}/\mathrm{d}t)\phi_{i,j}]. \tag{6}$$

As shown in fig. 1d, the magnetic resistances $R_{i+1/2}$, $R_{i-1/2}$, $R_{j+1/2}$, $R_{j-1/2}$ in eq. (6) are respectively decomposed into four magnetic resistances by the difference of permeabilities (see fig. 1b).

The magnetic resistance is generally defined by

$$\textit{magnetic resistance}=\frac{\textit{length of the flux path}}{\left[\begin{array}{c}\textit{permeability}\\ \textit{of the material}\end{array}\right]\left[\begin{array}{c}\textit{cross-sectional area}\\ \textit{normal to the flux path}\end{array}\right]}. \tag{7}$$

Some examples of magnetic resistance with typical shapes are listed in table 1. By the definition of eq. (7) it is possible to calculate the magnetic resistances $R_{x\mathrm{A}}$, $R_{z\mathrm{B}}$ in table 1. However, eq. (7) is not directly applicable to calculate the magnetic resistances $R_{x\mathrm{B}}$, $R_{y\mathrm{B}}$, $R_{x\mathrm{C}}$, $R_{y\mathrm{C}}$ because the length of the flux path or cross-sectional area normal to the flux path differs according to the positions. Therefore, for the second example in table 1 it is assumed that the magnetic resistance $R_{x\mathrm{B}}$ is composed of a large number of parallel-connected small magnetic resistances that are similar in shape to the magnetic resistance $R_{x\mathrm{A}}$. Also, it is assumed that the magnetic resistance $R_{y\mathrm{B}}$ in table 1 is composed of a large number of series-connected small magnetic resistances that are similar in shape to the magnetic resistance $R_{x\mathrm{A}}$. When the number of parallel- or series-connected magnetic resistances reach infinity, the calculations of magnetic resistances $R_{x\mathrm{B}}$, $R_{y\mathrm{B}}$ reduce to the evaluation of Riemann integrals (see [9]). Similarly, the magnetic resistances $R_{x\mathrm{C}}$, $R_{y\mathrm{C}}$ in table 1 are obtained by making assumptions similar to those used in calculating of $R_{x\mathrm{B}}$, $R_{y\mathrm{B}}$.

The electric resistance is generally defined by

$$\textit{electric resistance}=\frac{\textit{length of the current path}}{\left[\begin{array}{c}\textit{conductivity}\\ \textit{of the material}\end{array}\right]\left[\begin{array}{c}\textit{cross-sectional area}\\ \textit{normal to the current path}\end{array}\right]}. \tag{8}$$

By comparing eq. (7) with eq. (8), it is found that the parameter which depends on the shape is common eq. (7) to eq. (8). Thereby, the electric resistances which are similar in shape listed in table 1 are obtained by making assumptions similar to those used in calculating of magnetic resistances $R_{x\mathrm{B}}$, $R_{y\mathrm{B}}$, $R_{x\mathrm{C}}$, $R_{y\mathrm{C}}$.

In the region containing air the permeability μ is constant. However, in the region containing iron the permeability μ depends on the magnetic field intensity H at each position, that is

Table 1. Examples of magnetic resistances

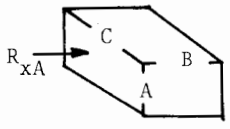

$$R_{xA} = \frac{B}{\mu AC}$$

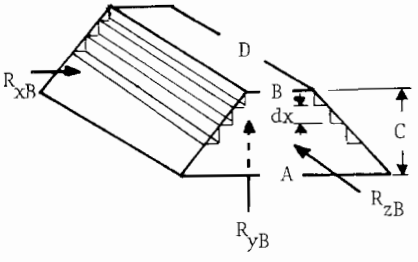

$$R_{xB} = \frac{1}{\mu D \int_0^C \frac{dx}{B + \{(A-B)/C\}x}} = \frac{A-B}{\mu CD \log(A/B)}$$

$$R_{yB} = \frac{1}{\mu D} \int_0^C \frac{dx}{B + \{(A-B)/C\}x} = \frac{C}{\mu D(A-B)} \log(A/B)$$

$$R_{zB} = \frac{2D}{\mu(A+B)C}$$

$$dx \simeq \Delta x = C/m$$

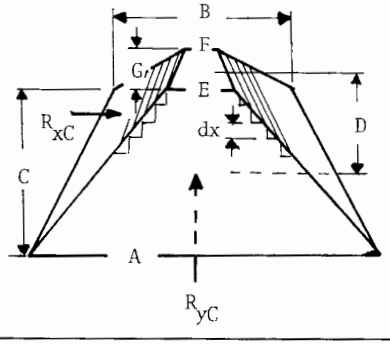

$$R_{xC} = \frac{1}{\mu \int_0^D \frac{G + \{(C-G)/D\}x}{E - F + \{(A-B+F-E)/D\}x} \log\left[\frac{E + \{(A-E)/D\}x}{F + \{(B-F)/D\}x}\right] dx}$$

$$R_{yC} = \frac{2}{\mu} \int_0^D \frac{dx}{[G + \{(C-G)/D\}x][E + F + \{(A+B-E-F)/D\}x]}$$

$$dx \simeq \Delta x = D/m$$

Note: Practical calculations of R_{xB}, R_{yB}, R_{xC}, R_{yC} were carried out by means of the numerical integration method for the sake of generality.

$$\mu = f(H), \tag{9}$$

where $f(H)$ denotes a function of H. By considering figs. 1b–1d, the magnetic field intensities H_{eb} and H_{bf} are calculated by means of the magnetic field energy relation. The magnetic field energy stored in the shadowed portion in fig. 1b is

$$w = \frac{1}{2}\mu_{i,j}^{(1)}(H_{eb}^2 + H_{bf}^2)V_{i,j}^{(1)} = \frac{1}{2}\left[R_i^{(1)}\left\{\frac{R_{i+1}^{(3)}}{R_i^{(1)} + R_{i+1}^{(3)}}(\phi_{i,j} - \phi_{i+1,j})\right\}^2 + R_j^{(1)}\left\{\frac{R_{j-1}^{(2)}}{R_j^{(1)} + R_{j-1}^{(2)}}(\phi_{i,j} - \phi_{i,j-1})\right\}^2\right], \tag{10}$$

where $V_{i,j}^{(1)}$ denotes the volume of the region taking the permeability $\mu_{i,j}^{(1)}$ in fig. 1b. The magnetic resistances $R_i^{(1)}$, $R_j^{(1)}$, $R_{i+1}^{(3)}$, $R_{j-1}^{(2)}$ and the loop magnetic fluxes $\phi_{i,j}$, $\phi_{i+1,j}$, $\phi_{i,j-1}$ are shown in figs. 1c and 1d.

By means of eq. (10) it is possible to obtain the magnetic field intensities H_{eb}, H_{bf} as

$$H_{eb} = \sqrt{\frac{R_i^{(1)}}{\mu_{i,j}^{(1)} V_{i,j}^{(1)}}} \frac{R_{i+1}^{(3)}}{R_i^{(1)} + R_{i+1}^{(3)}} (\phi_{i,j} - \phi_{i+1,j}), \tag{11}$$

$$H_{bf} = \sqrt{\frac{R_j^{(1)}}{\mu_{i,j}^{(1)} V_{i,j}^{(1)}}} \frac{R_{j-1}^{(2)}}{R_j^{(1)} + R_{j-1}^{(2)}} (\phi_{i,j} - \phi_{i,j-1}). \tag{12}$$

When eqs. (11) and (12) are substituted into eq. (9), then we can formally obtain the permeability $\mu_{i,j}^{(1)}$ of the shadowed portion in fig. 1b as a function of the magnetic fluxes and the permeabilities.

The permeabilities of the other portions in fig. 1b can be obtained in a similar manner.

2.2. Magnetic circuits of a saturable reactor

Most electromagnetic devices consist of the conducting wires wound around an iron core. A typical example of these electromagnetic devices is a saturable reactor as shown in fig. 2a.

At the time when the exciting current is flowing through the coil of the saturable reactor in fig. 2a, in order to minimize the magnetic field energy stored in the saturable reactor, the eddy currents in the iron core flow in a direction opposite to the exciting currents. On the other hand, the magnetic flux which passes through the path parallel to the current-carrying coil can be neglected; therefore, it is preferable to consider the solid element as shown in fig. 2b. The permeability of this solid element is determined from the magnetic field intensities in the tangential direction and in the radial direction. Also, the central portion of the solid element in fig. 2b is one of the elements, and the permeability of this element becomes a function of the magnetic field intensity in the tangential direction because the magnetic resistance in the radial direction reaches an infinitely large value. The magnetic resistances in fig. 2b correspond to those in table 1.

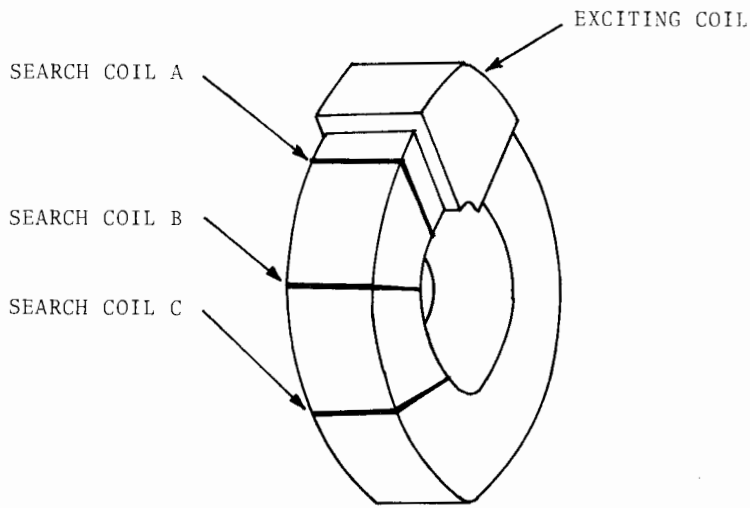

Fig. 2a. Magnetic circuit of a saturable reactor: schematic diagram of a saturable reactor.

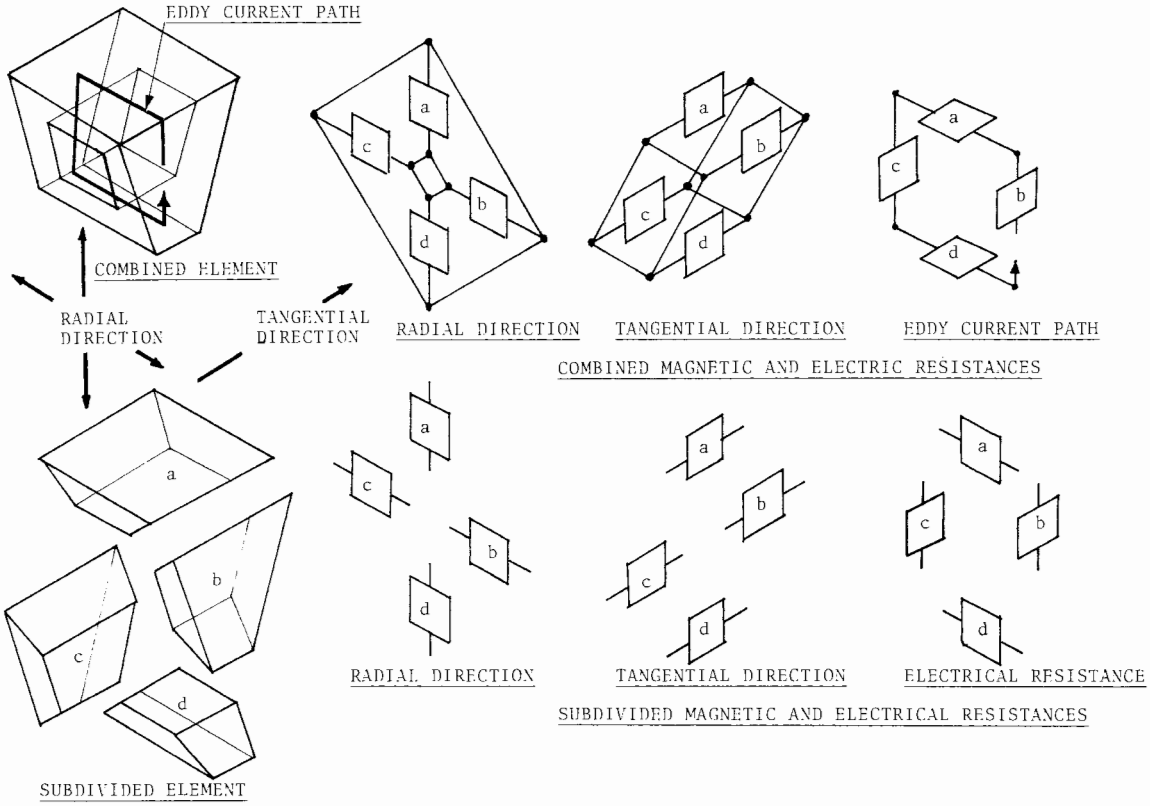

Fig. 2b. Magnetic circuit of a saturable reactor: solid element and its subdivided elements.

The saturable reactor shown in fig. 2a is subdivided in much the same way as the solid element shown in fig. 2b, taking into account the region containing air; thus for a saturable reactor the calculation of three-dimensional magnetic fields can be carried out in a two-dimensional coordinate system (which consists of the tangential and radial directions) without committing any appreciable error.

For simplicity, it is preferable to consider a concrete example. Therefore, the saturable reactor shown in fig. 2a is subdivided into three parts in the radial direction and two parts in the tangential direction. Moreover, it is assumed that no magnetic flux flows out of a region which is not taken into account by the calculation of magnetic fields. Fig. 2c shows the magnetic circuit of this example.

The magnetic system of equations is preferably expressed in matrix notation involving the externally impressed magnetomotive force vector $\boldsymbol{F}$ and the magnetic flux vector $\boldsymbol{\Phi}$. With $\boldsymbol{Z}$ denoting the magnetic impedance matrix, the magnetic system of equations in fig. 2c is given by means of eq. (6):

$$\boldsymbol{F} = \boldsymbol{Z}\boldsymbol{\Phi}. \tag{13}$$

The externally impressed magnetomotive force vector $\boldsymbol{F}$, which is a column matrix of order 4, is composed of the winding matrix $\boldsymbol{W}$, the electrical conductance matrix $\boldsymbol{G}$ and the

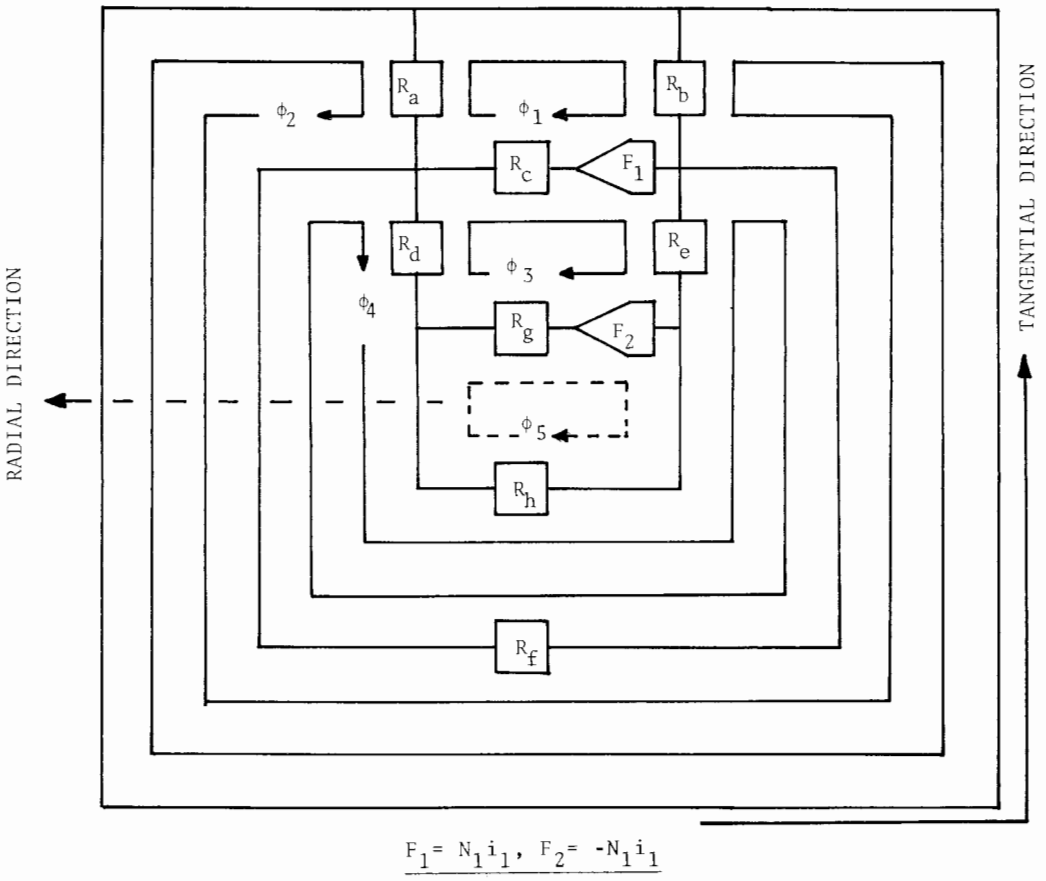

Fig. 2c. Magnetic circuit of a saturable reactor: an example of a circuit.

externally impressed voltage vector $\boldsymbol{E}$, that is

$$\boldsymbol{F} = \boldsymbol{WGE} = \left\{\frac{N_1}{r_1} e_1, 0, 0, 0\right\}, \tag{14}$$

where N_1, r_1 and e_1 denote respectively the number of turns in the exciting coil, the electric resistance of exciting coil and the externally impressed voltage. The above matrices and vector are given by

$$\boldsymbol{W} = \lceil N_1, 1, 1, 1 \rfloor, \tag{15}$$

$$\boldsymbol{G} = \left\lceil \frac{1}{r_1}, 0, \frac{1}{r_3}, \frac{1}{r_4} \right\rfloor, \tag{16}$$

$$\boldsymbol{E} = \{e_1, 0, 0, 0\}, \tag{17}$$

where r_3 and r_4 are respectively the electric resistances of the iron core related to the loop magnetic flux ϕ_3 and to the loop magnetic flux ϕ_4 in fig. 2c.

The magnetic impedance matrix $\boldsymbol{Z}$ is a linear combination of the magnetic resistance matrix $\boldsymbol{D}$ and the coefficient matrix $\boldsymbol{L}$:

$$\boldsymbol{Z} = \boldsymbol{D} + (\mathrm{d}/\mathrm{d}t)\boldsymbol{L}. \tag{18}$$

The matrix $\boldsymbol{D}$ is a square matrix of order 4 involving the magnetic resistances R_a, R_b, R_c, R_d, R_e, R_f, R_g, R_h of the magnetic circuits shown in fig. 2c, viz.

$$\boldsymbol{D} = \begin{bmatrix} R_1 & -R_{12} & -R_c & 0 \\ & R_2 & 0 & -R_f \\ & & R_3 & -R_{34} \\ & & & R_4 \\ \text{symmetric} & & & \end{bmatrix}, \tag{19}$$

where

$$\begin{aligned} R_1 &= R_a + R_b + R_c, \\ R_2 &= R_a + R_b + R_f, \\ R_3 &= R_c + R_d + R_e + R_g, \\ R_4 &= R_d + R_e + R_f + R_h, \\ R_{12} &= R_a + R_b, \\ R_{34} &= R_d + R_e. \end{aligned} \tag{20}$$

The coefficient matrix $\boldsymbol{L}$ is composed of the winding matrix $\boldsymbol{W}$ and the electrical conductance matrix $\boldsymbol{G}$, that is

$$\boldsymbol{L} = \boldsymbol{W}\boldsymbol{G}\boldsymbol{W} = \left[\frac{N_1^2}{r_1}, 0, \frac{1}{r_3}, \frac{1}{r_4}\right]. \tag{21}$$

By considering eqs. (13)–(21) and fig. 2c, it is found that the loop magnetic flux ϕ_5 must be taken into account in the calculation of magnetic fields to satisfy the condition of a minimum number of network equations [10]. Therefore, the loop magnetic flux ϕ_5 in fig. 2c can be added by use of the relationship (see appendix)

$$\boldsymbol{\Phi} = \boldsymbol{C}^{\mathrm{t}}\boldsymbol{\Phi}^c, \qquad \text{i.e.} \quad \begin{bmatrix} \phi_1 \\ \phi_2 \\ \phi_3 \\ \phi_4 \end{bmatrix} = \begin{bmatrix} 1 & 0 & 0 & 0 & -1 \\ 0 & 1 & 0 & 0 & -1 \\ 0 & 0 & 1 & 0 & -1 \\ 0 & 0 & 0 & 1 & -1 \end{bmatrix} \begin{bmatrix} \phi_1^c \\ \phi_2^c \\ \phi_3^c \\ \phi_4^c \\ \phi_5^c \end{bmatrix}, \tag{22}$$

where $\boldsymbol{\Phi}^c$ is the new magnetic flux vector and $\boldsymbol{C}$ is the magnetic flux connection matrix (superscript t denotes the transpose of the matrix, and c refers to transformed quantities).

Then the new magnetic system of equations is given by

$$\boldsymbol{F}^c = \boldsymbol{Z}^c \boldsymbol{\Phi}^c, \tag{23}$$

where

$$\boldsymbol{F}^c = \boldsymbol{C}\boldsymbol{F} = \left\{ \frac{N_1}{r_1} e_1, 0, 0, 0, -\frac{N_1}{r_1} e_1 \right\},$$

$$\boldsymbol{Z}^c = \boldsymbol{C}\boldsymbol{Z}\boldsymbol{C}^t = \boldsymbol{D}^c + (\mathrm{d}/\mathrm{d}t)\boldsymbol{L}^c,$$

$$\boldsymbol{D}^c = \boldsymbol{C}\boldsymbol{D}\boldsymbol{C}^t = \begin{bmatrix} R_1 & -R_{12} & -R_c & 0 & 0 \\ & R_2 & 0 & -R_f & 0 \\ & & R_3 & -R_{34} & -R_g \\ \text{symmetric} & & & R_4 & -R_h \\ & & & & R_g + R_h \end{bmatrix},$$

$$\boldsymbol{L}^c = \boldsymbol{C}\boldsymbol{L}\boldsymbol{C}^t = \begin{bmatrix} \frac{N_1^2}{r_1} & 0 & 0 & 0 & -\frac{N_1^2}{r_1} \\ & 0 & 0 & 0 & 0 \\ & & \frac{1}{r_3} & 0 & -\frac{1}{r_3} \\ & & & \frac{1}{r_4} & -\frac{1}{r_4} \\ \text{symmetric} & & & & \frac{N_1^2}{r_1} + \frac{1}{r_3} + \frac{1}{r_4} \end{bmatrix}. \tag{24}$$

The induced voltage vector $\boldsymbol{U}$ in electrical circuits depends on the rate of change of the linkage flux in time t, that is

$$\boldsymbol{U} = \{u_1, u_2, u_3, u_4\} = \boldsymbol{W}\boldsymbol{C}^t(\mathrm{d}/\mathrm{d}t)\boldsymbol{\Phi}^c. \tag{25}$$

The vector of current $\boldsymbol{I}$, which consists of the exciting current i_1 and the eddy currents i_2, i_3, i_4, is given in terms of the externally impressed voltage vector $\boldsymbol{E}$, the induced voltage vector $\boldsymbol{U}$ and the electrical conductance matrix $\boldsymbol{G}$, viz.

$$\boldsymbol{I} = \{i_1, i_2, i_3, i_4\} = \boldsymbol{G}(\boldsymbol{E} - \boldsymbol{U}). \tag{26}$$

By means of eqs. (23)–(26) it is possible to obtain the magnetodynamic fields, induced voltages and eddy currents in a saturable reactor.

2.3. Numerical method of solution

By means of eqs. (23) and (24) it is possible to write the magnetic system of equations as

$$\boldsymbol{L}^c(\mathrm{d}/\mathrm{d}t)\boldsymbol{\Phi}^c = -\boldsymbol{D}^c\boldsymbol{\Phi}^c + \boldsymbol{F}^c. \tag{27}$$

With Δt denoting the stepwidth, the finite difference representation of eq. (27) is given as

$$\boldsymbol{L}^c(1/\Delta t)(\boldsymbol{\Phi}^c_{t+\Delta t} - \boldsymbol{\Phi}^c_t) = -[\alpha \boldsymbol{D}^c_{t+\Delta t}\boldsymbol{\Phi}^c_{t+\Delta t} + (1-\alpha)\boldsymbol{D}^c_t\boldsymbol{\Phi}^c_t] + [\alpha \boldsymbol{F}^c_{t+\Delta t} + (1-\alpha)\boldsymbol{F}^c_t], \qquad (28)$$

where the parameter α can be chosen arbitrarily (e.g. $\alpha = 0$, $\alpha = 1/2$, $\alpha = 1$ yield forward, central, backward differences), and subscripts t and $t+\Delta t$ refer to the times t and $t+\Delta t$, respectively. By rearrangement, eq. (28) reduces to

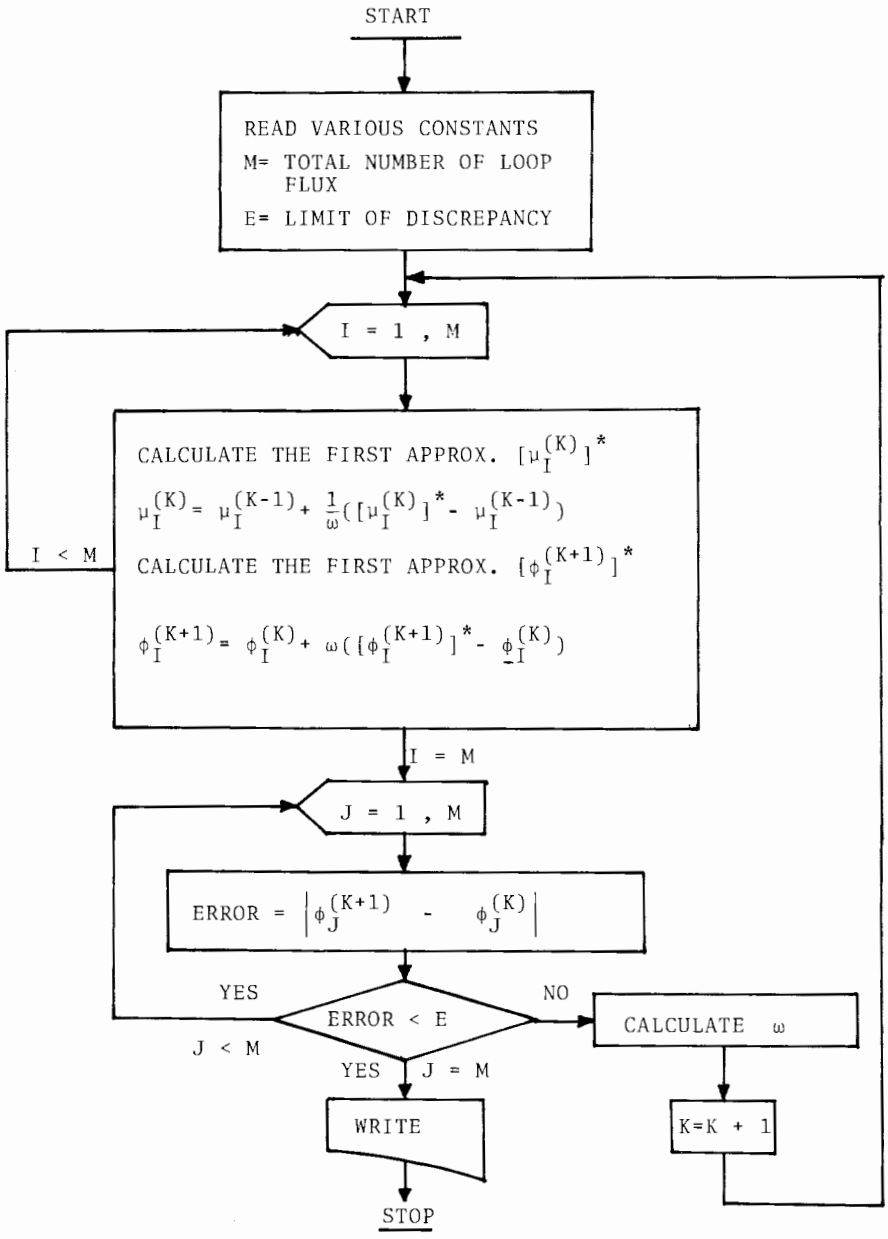

Fig. 3. Flow chart of the iteration method.

$$[(1/\Delta t)\boldsymbol{L}^c + \alpha \boldsymbol{D}^c_{t+\Delta t}]\boldsymbol{\Phi}^c_{t+\Delta t} = [(1/\Delta t)\boldsymbol{L}^c - (1-\alpha)\boldsymbol{D}^c_t]\boldsymbol{\Phi}^c_t + [\alpha \boldsymbol{F}^c_{t+\Delta t} + (1-\alpha)\boldsymbol{F}^c_t]. \tag{29}$$

Since the magnetic circuit equation that takes into account the nonlinear magnetization characteristic of iron is one of the nonlinear algebraic equations, the calculation of the magnetic flux vector $\boldsymbol{\Phi}^c_{t+\Delta t}$ in eq. (29) reduces to the solution of a system of simultaneous nonlinear algebraic equations. This system is solved by iteration, using a relaxation parameter, which is sequentially determined in every complete iteration by the method described in [9]. Fig. 3 shows the flow chart of this iteration method.

By the application of the central difference method to eqs. (25) and (26) the induced voltage vector $\boldsymbol{U}_{t+\Delta t/2}$ and the current vector $\boldsymbol{I}_{t+\Delta t/2}$ are given by

$$\boldsymbol{U}_{t+\Delta t/2} = \boldsymbol{W}\boldsymbol{C}^t(1/\Delta t)(\boldsymbol{\Phi}^c_{t+\Delta t} - \boldsymbol{\Phi}^c_t), \tag{30}$$

$$\boldsymbol{I}_{t+\Delta t/2} = \boldsymbol{G}(\boldsymbol{E}_{t+\Delta t/2} - \boldsymbol{U}_{t+\Delta t/2}), \tag{31}$$

where the subscript $t + \Delta t/2$ refers to the time $t + \Delta t/2$.

3. Numerical solution

Various constants used in the calculation of the saturable reactor shown in fig. 2a are listed in table 2. Fig. 4 shows the nonlinear magnetization characteristic of iron. In carrying out the magnetic field calculation of the saturable reactor, the nonlinear magnetization characteristic of the iron part of the reactor is introduced by linear interpolation [11].

At first, we have to decide the appropriate value of α in eq. (28). For comparison, the transient magnetic fluxes were calculated by the methods of forward differences ($\alpha = 0$), central differences ($\alpha = 1/2$) and backward differences ($\alpha = 1$). Among the results obtained by each method the numerical solutions computed by the backward difference method were somewhat small compared with the results obtained by the central difference method. On the contrary, the forward difference method produced so instable solution that this method

Table 2. Various constants used in the calculation

Number of subdivisions in radial direction	8
Number of subdivisions in tangential direction	12
Limit of discrepancy	0.1 percent
Inner radius of iron core	0.025 [m]
Outer radius of iron core	0.035 [m]
Thickness of iron core	0.01 [m]
Thickness of exciting coil	0.003 [m]
Thickness of the region containing air	0.017 [m]
Number of turns of exciting coil	100 turns
Number of turns of search coils	25 turns
Electric resistance of exciting coil	1.21 [Ω]
Conductivity of iron core (cast iron)	1/80 [1/μΩ cm]
Externally impressed voltage (step voltage)	5.0 [V]

All the initial magnetic fluxes and currents are set to be zero.

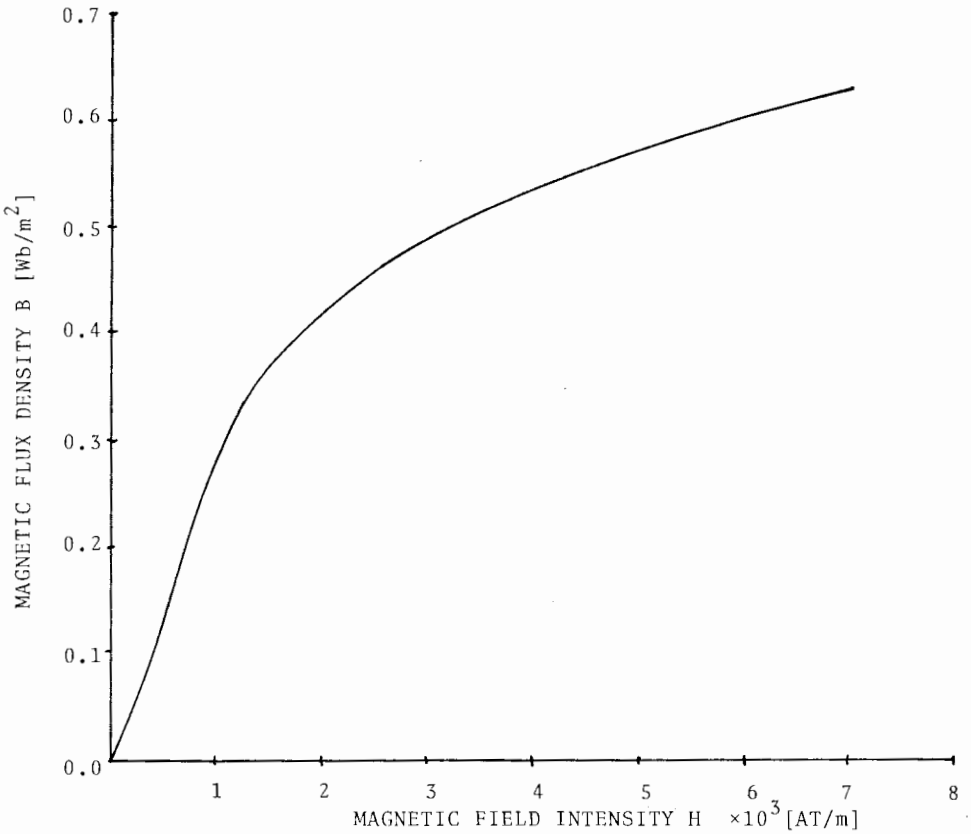

Fig. 4. Nonlinear magnetization characteristic of iron ($\mu = B/H$).

became useless. Therefore, in this paper the magnetodynamic field calculations of the saturable reactor were carried out by means of the central difference method.

Second, numerical tests using various stepwidths were carried out. Typical results of the tests are summarized in fig. 5. When we consider the results of fig. 5, we can find that the solutions using the stepwidth $\Delta t = 0.0005$ (sec) have satisfactory accuracy.

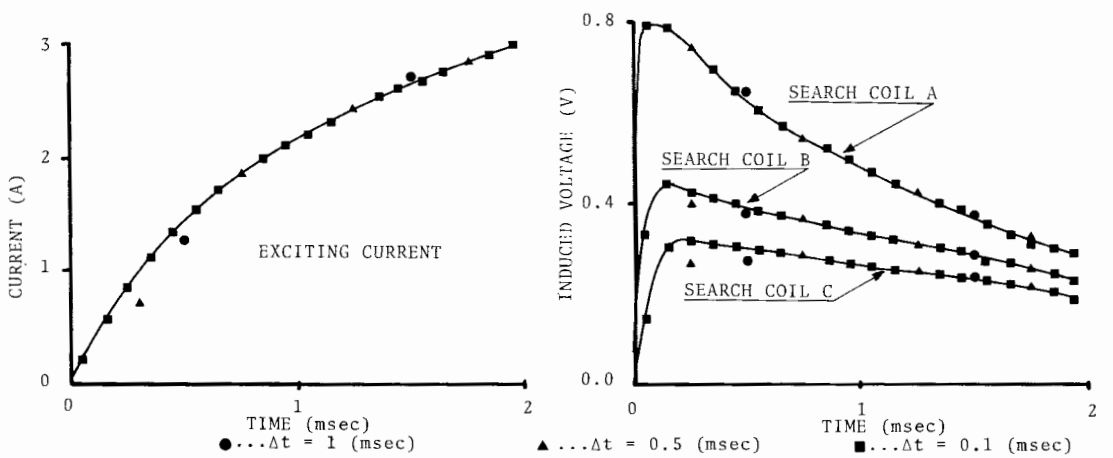

Fig. 5. Typical results of the numerical tests using various stepwidths.

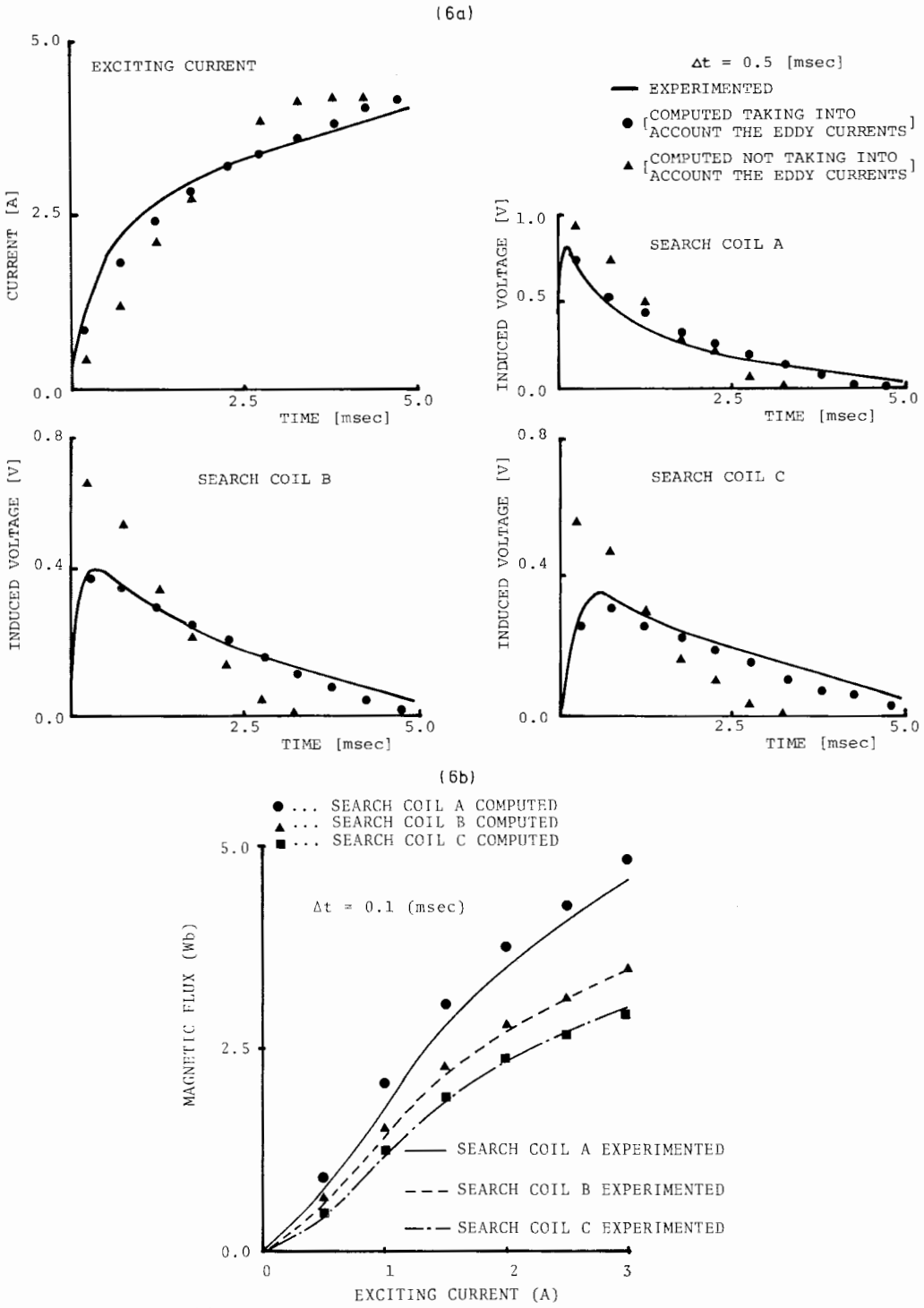

Fig. 6. Numerical solutions. (a) exciting current and induced voltages at the search coils from the transient to the steady states, (b) the relationship between steady state exciting currents and magnetic fluxes calculated under six different step voltages.

Third, we continued the numerical calculation until the numerical solutions reached the steady state values. As shown in fig. 6a, the exciting current reached the steady state value and the induced voltages at the search coils reduced to zero. Fig. 6b shows the relationship between steady state exciting currents and magnetic fluxes together with the experimental values. The numerical calculations were carried out under six different step voltages so that the results shown in fig. 6b were obtained. The experimental values in fig. 6b were obtained by integrating the induced voltages at the search coils by an electronic integrator [12].

Finally, the initial transient exciting current and induced voltages at the search coils are shown in fig. 7 together with the experimental results. In order to perform a good switching operation, a simple electronic switching circuit (fig. 8) utilizing a silicon-controlled rectifier was used. As shown in fig. 8, the input step voltage wave form is of fairly good accuracy. Therefore, the stepwidth was not changed at the beginning of numerical calculation. Also, the experimental results in fig. 6a were obtained by the simple test circuit shown in fig. 8.

When we consider the results of figs. 6a and 7, it is obvious that the magnetodynamic fields in the saturable reactor are considerably dominated by the eddy currents flowing through the iron core.

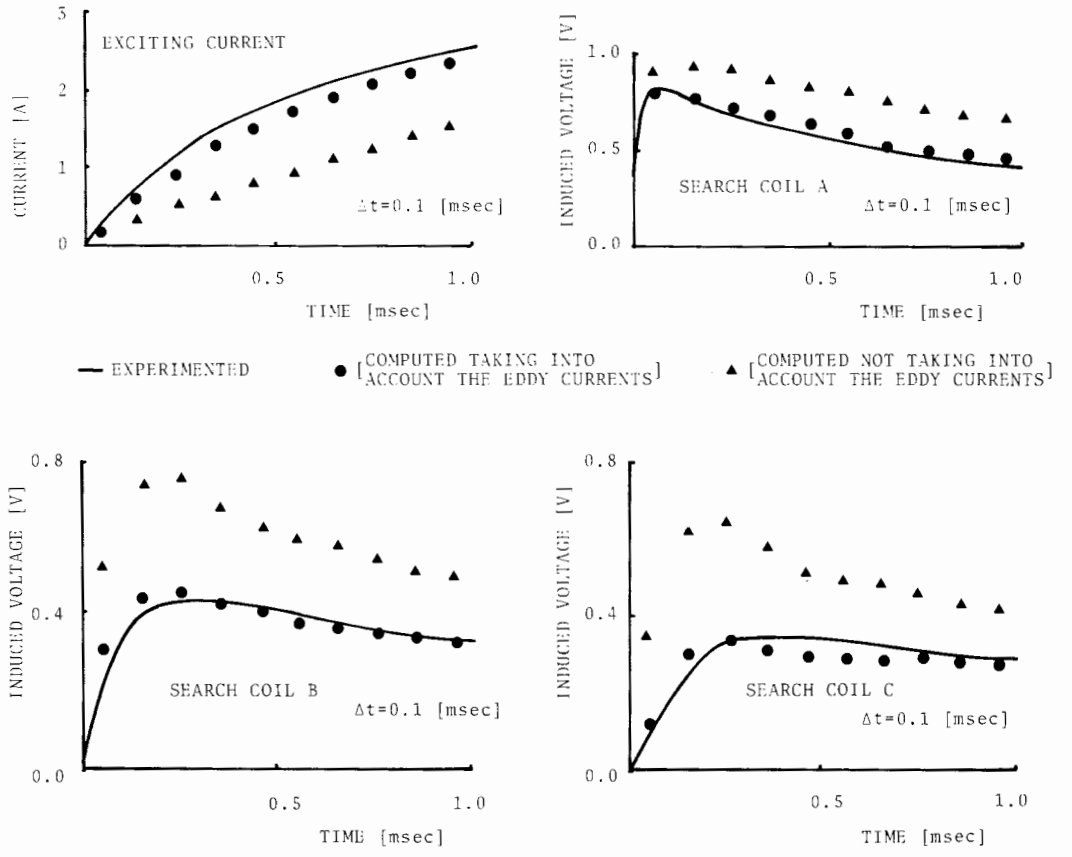

Fig. 7. Transient exciting current and induced voltages at the search coils.

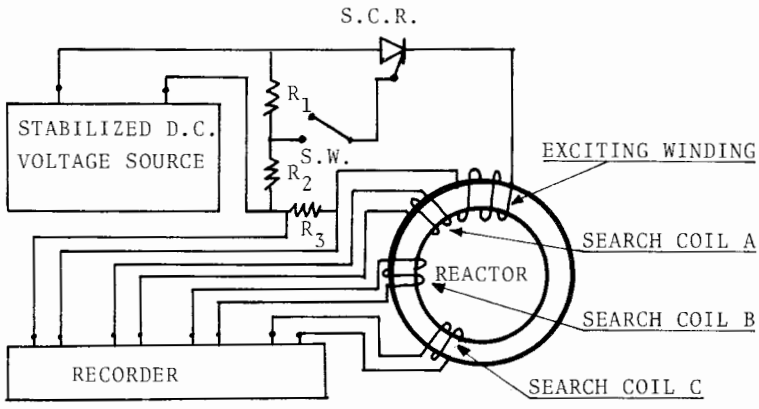

Fig. 8. Schematic diagram of the experiment and the experimentally used input voltage source wave form.

4. Conclusion

In this paper, it has been shown that the method of magnetic circuits is quite effectively applicable to the magnetodynamic field problems in electromagnetic devices. Consequently, three-dimensional magnetodynamic fields of a saturable reactor have been predetermined, taking into account the eddy currents. Moreover, it has been shown that the system of magnetic circuit equations is effectively solved by the central difference method along with the iteration method.

The operation count required to obtain the results of fig. 7 was about 10 minutes on the computer FACOM 230–45S.

Acknowledgement

The author is grateful to Professor I. Fujita and Professor T. Yamamura for their helpful advice and to Professor T. Nishiya for the facilities given by him at the computer center of Hosei University. The assistance of Mr. S. Hayano is gratefully acknowledged.

Appendix. Coordinate transformation

The magnetic field energy stored in the saturable reactor is constant, regardless of the coordinate system. Therefore, the magnetic field energy in the original coordinate system must be equivalent to the magnetic field energy in the transformed coordinate system, that is

$$\boldsymbol{\Phi}^{\mathrm{t}}\boldsymbol{F} = (\boldsymbol{\Phi}^{c})^{\mathrm{t}}\boldsymbol{F}^{c}, \tag{A.1}$$

or

$$\boldsymbol{\Phi}^{\mathrm{t}}\boldsymbol{Z}\boldsymbol{\Phi} = (\boldsymbol{\Phi}^{c})^{\mathrm{t}}\boldsymbol{Z}^{c}\boldsymbol{\Phi}^{c}. \tag{A.2}$$

The magnetic flux vector $\boldsymbol{\Phi}$ and the transformed magnetic flux vector $\boldsymbol{\Phi}^{c}$ are related by

$$\boldsymbol{\Phi} = \boldsymbol{C}^{\mathrm{t}}\boldsymbol{\Phi}^{c}. \tag{A.3}$$

When eq. (A.3) is substituted into eqs. (A.1) and (A.2), we obtain

$$(\boldsymbol{C}^{\mathrm{t}}\boldsymbol{\Phi}^{c})^{\mathrm{t}}\boldsymbol{F} = (\boldsymbol{\Phi}^{c})^{\mathrm{t}}\boldsymbol{F}^{c}, \tag{A.4}$$

$$(\boldsymbol{C}^{\mathrm{t}}\boldsymbol{\Phi}^{c})^{\mathrm{t}}\boldsymbol{Z}(\boldsymbol{C}^{\mathrm{t}}\boldsymbol{\Phi}^{c}) = (\boldsymbol{\Phi}^{c})^{\mathrm{t}}\boldsymbol{Z}^{c}\boldsymbol{\Phi}^{c}. \tag{A.5}$$

By means of eqs. (A.4) and (A.5) it is possible to obtain the following relations:

$$\boldsymbol{F}^{c} = \boldsymbol{C}\boldsymbol{F}, \tag{A.6}$$

$$\boldsymbol{Z}^{c} = \boldsymbol{C}\boldsymbol{Z}\boldsymbol{C}^{\mathrm{t}}. \tag{A.7}$$

References

[1] F.C. Trutt, E.A. Erdelyi and R.F. Jackson, The nonlinear potential equation and its numerical solution for highly saturated electrical machines, IEEE Trans. Aerospace AS-1 (1963) 430–440.

[2] E.A. Erdelyi, S.V. Ahamed and R.D. Burtness, Flux distribution in saturated DC machines at no-load, IEEE Trans. Power Apparatus and Systems PAS-84 (1965) 375–381.

[3] S.V. Ahamed and E.A. Erdelyi, Flux distribution in DC machines on-load and overloads, IEEE Trans. Power Apparatus and Systems PAS-85 (1966) 960–967.

[4] E.A. Erdelyi, M.S. Sarma and S.S. Coleman, Magnetic fields in nonlinear salient pole alternator, IEEE Trans. Power Apparatus and Systems PAS-87 (1968) 1848–1856.

[5] E.A. Erdelyi and E.F. Fuchs, Nonlinear magnetic field analysis of DC machines, IEEE Trans. Power Apparatus and Systems PAS-89 (1970) 1546–1554.

[6] P. Silvester and M.V.K. Chari, Finite element solution of saturable magnetic field problems, IEEE Trans. Power Apparatus and Systems PAS-89 (1970) 1642–1651.

[7] A. Foggia, J.C. Sabonnadiere and P. Silvester, Finite element solution of saturated travelling magnetic field problems, IEEE Trans. Power Apparatus and Systems PAS-94 (1975) 866–871.

[8] Y. Saito, Method of magnetic circuits for nonlinear magnetostatic fields in polyphase induction motors at no-load, Comp. Meths. Appl. Mech. Eng. 13 (1978) 105–118.

[9] Y. Saito, Three-dimensional analysis of nonlinear magnetostatic fields in a saturable reactor. Comp. Meths. Appl. Mech. Eng. 16 (1978) 101–115.

[10] M.E. Van Valkenburg, Network analysis (Prentice-Hall, Englewood Cliffs, NJ, 1964).
[11] F.C. Trutt, E.A. Erdelyi and R.E. Hopkins, Representation of the magnetization characteristic of DC machines for computer use, IEEE Trans. Power Apparatus and Systems PAS-87 (1968) 665–669.
[12] N.R. Scott, Electronic computer technology (McGraw-Hill, New York, 1970).